ARTICLE

Fullerene-Conjugated Doxorubicin in Cells

Jia-Hui Liu,[†,‡] Li Cao,[†] Pengju G. Luo,[*,†] Sheng-Tao Yang,[†,‡] Fushen Lu,[†] Haifang Wang,[*,§] Mohammed J. Meziani,[†] Sk. Anwarul Haque,[†] Yuanfang Liu,[‡,§] Sebastian Lacher,[†] and Ya-Ping Sun[*,†]

Department of Chemistry and Laboratory for Emerging Materials and Technology, Clemson University, Clemson, South Carolina 29634-0973, Beijing National Laboratory for Molecular Sciences, College of Chemistry and Molecular Engineering, Peking University, Beijing 100871, China, and Institute of Nanochemistry and Nanobiology, Shanghai University, Shanghai 200444, China

ABSTRACT The conjugation of fullerene with well-established drug molecules has been a representative strategy to impart fullerene-specific properties for improved formulation. However, conjugates involving fullerenes or other nanomaterials often differ significantly from the free drug molecules in cellular uptake and distributions. For the highly effective anticancer drug doxorubicin (DOX), its strong absorption and fluorescence in the visible spectral region enable the tracking of DOX-containing conjugates by optical techniques. In this work, a stoimetrically and structurally well-defined fullerene-DOX conjugate was studied in terms of fluorescence microscopy, including the fluorescence imaging with two-photon excitation, to examine the uptake and distribution in human breast cancer cells. The results suggested that the conjugate was distributed mostly in the cytoplasm, significantly different from free DOX molecules (predominantly in the cell nucleus, as already reported in the literature). Mechanistic implications of the results are discussed. Also discussed are potentials of conjugated DOX species as self-labeled fluorescent probes in bioimaging and other mechanistic investigations on drug delivery.

KEYWORDS: fullerenes • doxorubicin • conjugates • fluorescence • bioimaging • cells

INTRODUCTION

Carbon nanomaterials including fullerenes and nanotubes have been studied extensively targeting their potential biological applications, though the emphases have been different between fullerenes and nanotubes to take advantage of their respective characteristics (1, 2). For fullerenes, the uniquely compact and spherical molecular structure has been exploited, so have been the distinctive electronic properties of fullerenes including especially their electron affinity (1). For example, C_{60} and derivatives were studied for their efficient quenching of various free radicals and reactive oxygen species (3), thus potentially serving as radical scavengers and/or anti-oxidatants in biological systems in vitro and in vivo (4−7). Among more specific examples was the use of fullerenes to inhibit oxidation-induced neuronal or cerebella granule cell death (5), prevent cell death associated with levodopa (6), and protect the liver from radical-related toxicity of carbon tetrachloride in rats (7).

The conjugation of fullerenes with well-established drug molecules has been a representative strategy to impart fullerene-specific properties for improved formulation (8−11). For the clinically highly effective anticancer drug paclitaxel, Wilson and coworkers synthesized covalent conjugate with C_{60} for a lipophilic slow-release system to enhance therapeutic efficacy (8). Their results suggested that the conjugate was similar to free paclitaxel in anti-tumor potency in vitro. Doxorubicin (DOX) is another highly effective drug in cancer chemotherapy, for which conjugates with fullerenes and carbon nanotubes have been pursued for purposes ranging from mitigating DOX-induced toxic side-effects (12−14) to improving the drug delivery for enhanced cellular uptake, selectivity to cancer cells, and pH regulated release (15−18). Recently, a methano-C_{60} derivative with hydrophilic spacers covalently tethered to two DOX units (Scheme 1) was prepared to render the resulting conjugate aqueous compatible (11). The anti-neoplastic activities of DOX were apparently preserved in the conjugate according to evaluations in vitro with human breast cancer cells (11).

DOX is colored, with significant fluorescence in the visible spectral region (15, 18). The optical properties provide opportunities to track DOX molecules and conjugates by using fluorescence-based techniques, such as assessing nano-carrier of DOX in cells without any other fluorescence labels (17, 19, 20), or distributions of DOX and the carrier (with a separate fluorescence label) (15). Here we report a study that took advantage of the optical functions of DOX, including the use of two-photon fluorescence imaging, to examine the uptake and distribution of the stoimetrically and structurally well-defined and aqueous compatible fullerene-DOX conjugate (Scheme 1) in cells. Mechanistic implications of the results are discussed.

RESULTS AND DISCUSSION

The fullerene-DOX conjugate was structurally built upon a methano-C_{60} derivative, to which two DOX molecules were

* To whom correspondence should be addressed. E-mail: pluo@clemson.edu, hwang@shu.edu.cn, and syaping@clemson.edu.
Received for review January 14, 2010 and accepted April 13, 2010
† Clemson University.
‡ Peking University.
§ Shanghai University.
DOI: 10.1021/am100037y

Published on Web 04/26/2010

Scheme 1

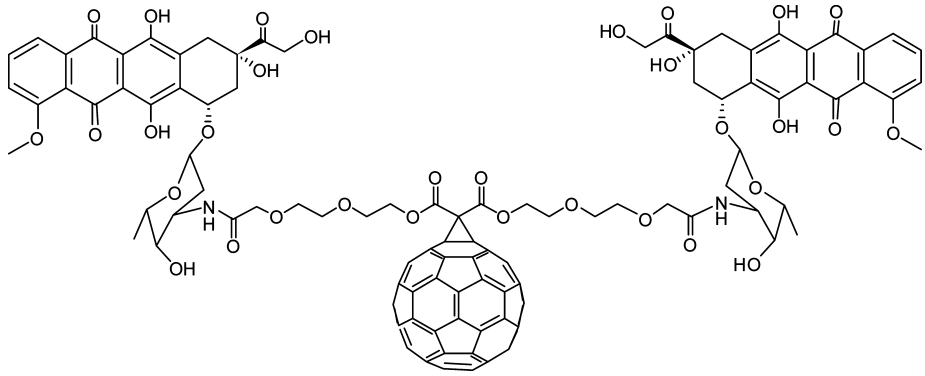

covalently linked through hydrophilic spacers (Scheme 1) for aqueous compatibility. The synthesis of the conjugate and unambiguous characterizations of the conjugate structure and properties such as solubility characteristics have been reported (11). Spectroscopically, the observed absorption spectrum of the conjugate was close to a superposition of those of free DOX and methano-C_{60} (Figure 1), with the latter being rather similar among a large collection of the C_{60} derivatives (21). Therefore, the absorption near the observed spectral peak (Figure 1) was due primarily to that of the DOX moieties in the conjugate. Methano-C_{60} derivatives are known to be only weakly fluorescent in the near-IR (quantum yields on the order of 1×10^{-3} to 1×10^{-4}) (21), no competition to the relatively stronger DOX fluorescence in the visible (quantum yield ~5%). However, in the conjugate the fluorescence from DOX moieties was quenched by the fullerene cage via intramolecular excited-state energy transfer, rather similar to that found in the structurally analogous fullerene-pyrene conjugate (22). The fluorescence quenching due to energy transfer in these conjugates is generally static in nature (23, 24), namely the emissive species and the quencher are in close proximity to result in an ultrafast quenching process (not subject to the limit of diffusion control) (22–24).

Despite the intramolecular quenching (Figure 1), which reduced the fluorescence quantum yield of the conjugated DOX species in solution to about 1.5%, the observed emissions with excitation into the visible (such as 458 nm, the commonly used wavelength for argon ion laser) in the fullerene-DOX conjugate were still overwhelmingly dominated by the DOX moieties (Figure 1). The conjugate could obviously serve as a nice fluorescence probe in bioimaging, not only for the bright fluorescence even in the presence of the quenching but also for the potential release of DOX from the conjugate (including conformational changes in the conjugate that would distance the DOX moieties from the fullerene cage) to result in substantially enhanced fluorescence intensities.

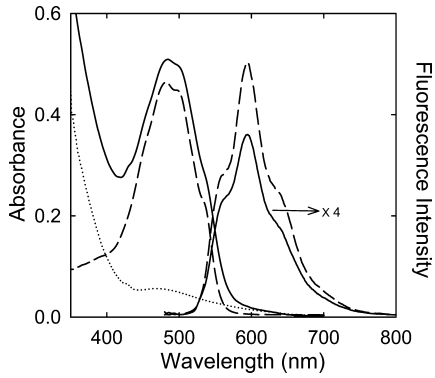

FIGURE 1. Absorption (left) and fluorescence (right, 458 nm excitation) spectra of DOX-HCl (- - -), the conjugate (—), and methanofullerene (· · · · ·) in DMSO solutions.

The conjugate and commercially supplied DOX sample (the HCl salt) in solutions were incubated with human breast cancer MCF-7 cells in a protocol similar to that used for the cytotoxicity assays (11). The DOX-equivalent concentration in the conjugate solution was matched by the free DOX solution for comparison in terms of absorption measurements (500 nm, Figure 1). Before imaging, the live cells were washed carefully for the removal of free DOX or conjugate species detached from the cells. The confocal fluorescence imaging was performed by using argon ion laser for excitation at 458 nm. The free DOX could readily be internalized by MCF-7 cells (Figure 2), as known in the literature (25), and so could the conjugate (Figure 3). Fluorescence spectra from the live cells were collected in situ on the confocal microscope to confirm that the emissions were indeed due to the internalized DOX species. In the cells the relative fluorescence intensities of the conjugate were generally lower than those of free DOX, consistent with the solution-phase results on the presence of intramolecular quenching in the conjugate. However, the quenching in cells seemed not as substantial as in solution, probably reflecting some conformational changes in the internalized conjugate that are less favorable to the mostly static energy transfer (donor and acceptor in close proximity) quenching process. In fact, if there were fewer conjugated DOX molecules internalized than free DOX molecules, as one might expect, the decrease in intramolecular fluorescence quenching in the internalized conjugates could be more significant.

Also shown in Figures 2 and 3 are confocal fluorescence images at a high resolution, which suggest that the distribution of the conjugate in cell was quite different from that of free DOX. For the latter, there was clearly a substantial accumulation in the cell nucleus, with only relatively weak fluorescence observed in the cell membrane or cytoplasm (Figure 2). The observation is generally consistent with what is known in the literature (20, 25). In fact, the ready uptake

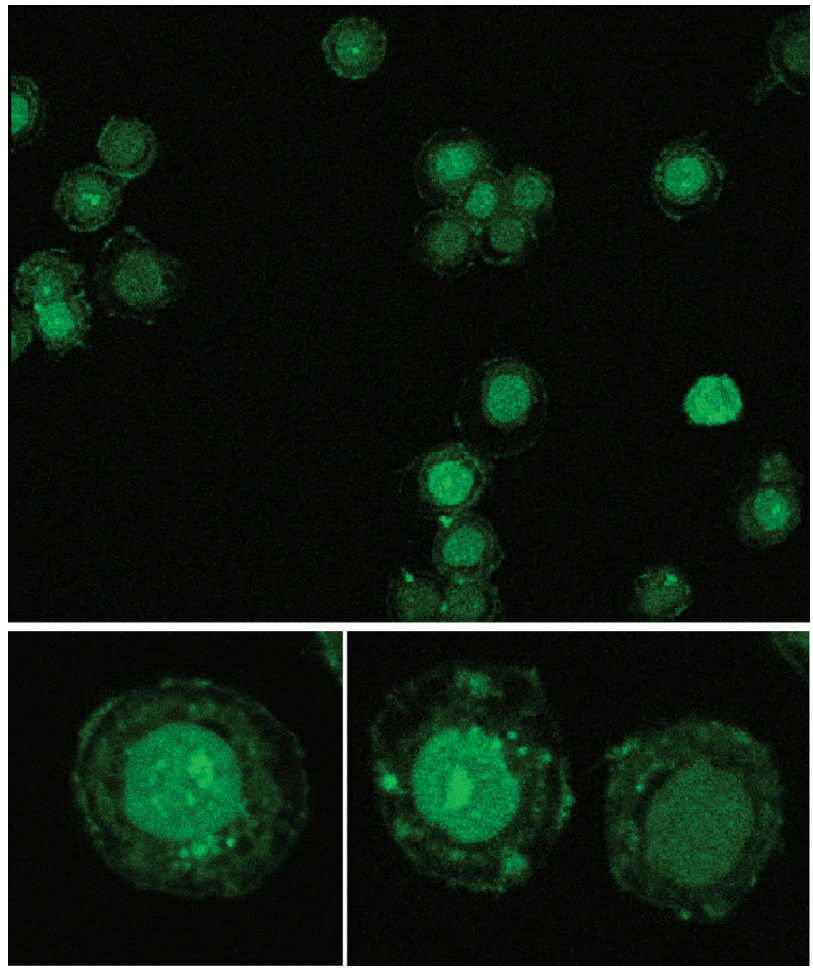

FIGURE 2. Confocal fluorescence imaging results (458 nm excitation) on free DOX in human breast cancer MCF-7 cells (upper), and similar results obtained at a higher resolution (lower).

of DOX by cell nucleus has served as evidence for the widely acknowledged mechanism on the anti-neoplastic function of this drug (26). In contrast, the internalized conjugate was found mostly in the cytoplasm (probably in endosomes and lysosomes, where nanoscale species are often found upon endocytosis), with weaker fluorescence from the cell nucleus (Figure 3). The different cellular distributions of the conjugate vs free DOX could be viewed more clearly in a three-dimensional fashion in images on different layers of the same cell (varying the *z*-axis in the confocal fluorescence imaging, see videos in the Supporting Information). The difference may at least in part be attributed to the presence of C_{60} cage in the conjugate structure. There has in fact already been precedence in the literature concerning the inhibitive effects of the fullerene cage on the uptake by cell nucleus. For example, Chaudhuri et al. reported that water-soluble fullerenols (with FITC as a fluorescence label) in cells were mostly localized within the lysosomal compartment (17).

DOX was found to be strongly two-photon active, namely that bright fluorescence could be observed with two-photon excitation of DOX in the near-IR (800−880 nm). Therefore, DOX may serve as an excellent two-photon fluorescence probe, as hinted in the literature (27). Two-photon fluorescence imaging is advantageous in terms of deeper penetration for thicker specimen due to dramatically reduced light scattering effects (28). The near-IR light for two-photon excitation is also less phototoxic owing to a lack of significant endogenous absorbers in most tissues (28). The low tissue absorbance of near-IR light and the generally non-invasive nature of two-photon excitation have promoted major advances of two-photon fluorescence imaging in biology and medicine (28−30).

The live MCF-7 cells from separate incubations with the conjugate and free DOX were imaged by two-photon excitation with a femtosecond pulsed laser at 800 nm. The results, confirming again the cellular uptake of both the conjugate and free DOX (Figure 4), were generally similar to those from the confocal fluorescence imaging, including the fluorescence brightness. Therefore, DOX moieties may indeed serve as excellent two-photon fluorescence probes in bioimaging and/or tracking drug delivery that require deeper tissue penetration.

DOX as the most commonly used anthracycline antitumor drug contains a planar aglycone moiety in the molecular structure. According to a more widely discussed mechanism for the tumor cytotoxicity (26), the planar aglycone moiety first intercalates into DNA in the cell nucleus, which induces DNA damages mediated by topoisomerase II (31) and modifies the ability of nuclear helicases to dissociate duplex DNA into single strands (thus hindering the process of strand

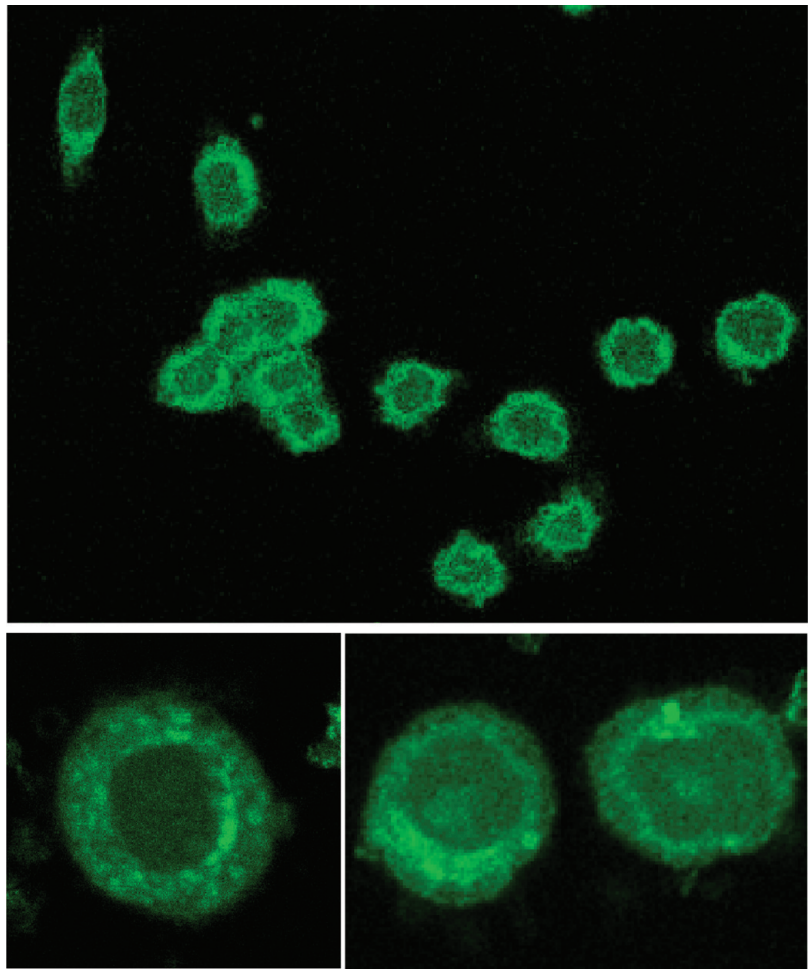

FIGURE 3. Confocal fluorescence imaging results (458 nm excitation) on the conjugate in human breast cancer MCF-7 cells (upper), and similar results obtained at a higher resolution (lower).

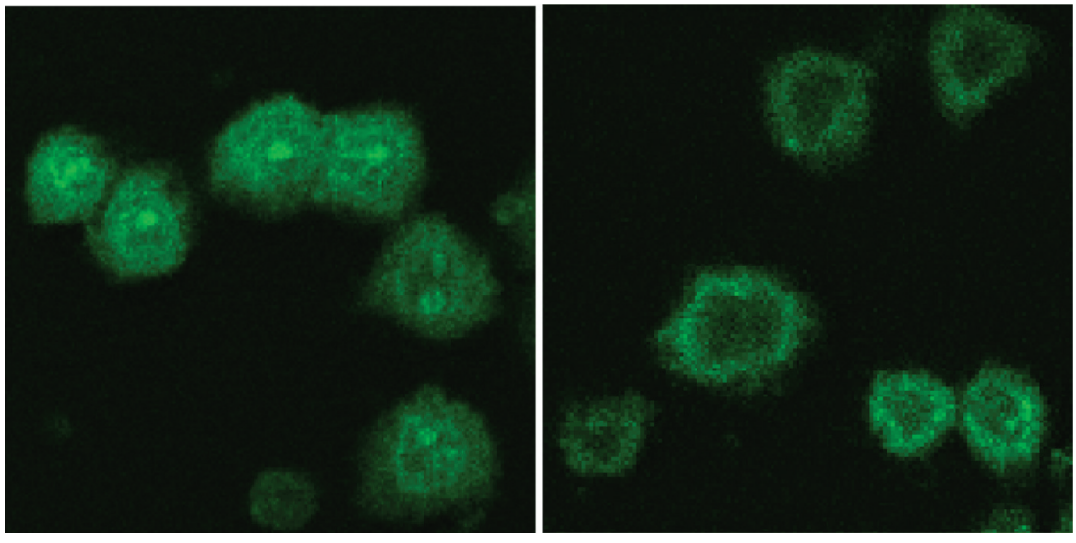

FIGURE 4. Two-photon fluorescence images (femtosecond pulsed excitation at 800 nm) on free DOX (left) and the conjugate (right) in human breast cancer MCF-7 cells.

separation) (32). In such a mechanistic framework, the obviously more favorable distribution of free DOX in the cell nucleus justifies the observed high cytotoxicity (19, 20, 25). However, the same mechanism may not be applicable to the similarly significant tumor cytotoxicity found for the fullerene-DOX conjugate (11). According to previous studies (20, 33, 34), DOX conjugates distributed mostly outside the cell nucleus may follow alternative mechanisms for tumor cytotoxicty, namely that nuclear accumulation may not be a prerequisite for the anti-neoplastic activities of DOX species. For example, Gillies, et al. reported that cells exposed to DOX-loaded micelles exhibited punctate fluorescence

mostly concentrated in the cytoplasm (20). Separately, transferrin-DOX conjugates were also found to distribute predominantly in cytoplasmic regions (similar to the fullerene-DOX conjugate), but their observed cytotoxicity was actually higher than that of free DOX (33). According to Kratz et al., the anti-tumor efficacy of the transferrin-DOX conjugate was related to the conjugate stability at lower pH (34), implying an interesting possibility for the conjugate resided in the cytoplasm to release free DOX gradually (thus conforming in part to the widely discussed mechanism of topoisomerase II inhibition in the cell nucleus 26, 31, 32).

Among alternative mechanisms proposed in the literature for the tumor cytotoxicity of DOX include the modulation of membranes, the extensive structural damage to mitochondria directly, the generation of cytotoxic free radical species, non-protein-associated DNA strand break, and the inducing of cell apoptosis (26, 33). Whether one or more of these mechanisms contributed significantly to the observed tumor cytotoxicity of the fullerene-DOX conjugate and other similar conjugates (34, 35) or the like (20) that distributed mostly outside the cell nucleus remains a fundamentally and practically important issue for further investigations. Obviously, the self labeling function of DOX with strong one- and two-photon fluorescence is highly valuable in such investigations. The presence of fluorescence quenching due to intramolecular energy transfer in the conjugate may actually be valuable to its serving as a fluorescent probe. The suppressed fluorescence intensities could be recovered completely or substantially upon the DOX species being dissociated from the conjugate or moved away from the fullerene cage, respectively, because of changes in the cellular environment, conceptually and phenomenologically similar to what have been widely studied for molecular beacon probes (36).

In summary, the fullerene-DOX conjugate as a stoichiometrically uniquely defined and structurally unambiguously characterized fluorescent probe was found to be readily uptaken by human breast cancer MCF-7 cells. The one- and two-photon fluorescence imaging results both confirmed that the conjugate was distributed mostly in the cytoplasm, thus establishing another solid example for comparable cytotoxicity of the conjugate with that of free DOX without the conjugate being predominantly in the cell nucleus. The conjugate as a fluorescent probe and the imaging results may prove valuable to the pursuit of a clearer mechanistic understanding of the DOX cytotoxicity.

EXPERIMENTAL SECTION

Materials. Doxorubicin hydrochloride (DOX-HCl) was purchased from BioChemica (Fluka), and DMSO from Sigma-Aldrich. Human breast adenocarcinoma cell line MCF-7 was obtained from Dr. G. Huang in Department of Biological Sciences at Clemson University.

The fullerene-DOX conjugate (Scheme 1) was synthesized and unambiguously characterized as reported previously (11). The aqueous compatibility of the conjugate was further confirmed as being adequate for bioevaluations in vitro.

Measurements. UV/vis absorption spectra were recorded on a Shimadzu UV2101-PC spectrophotometer. Fluorescence spectra were measured on a Spex Fluorolog-2 emission spectrometer equipped with a 450 W xenon source and a detector consisting of a Hamamatsu R928P photomultiplier tube operated at 950 V. Leica laser scanning confocal fluorescence microscope (DM IRE2, with Leica TCS SP2 SE scanning system) equipped with an argon ion laser (JDS Uniphase) and a femtosecond pulsed Ti:sapphire laser (Spectra-Physics Tsunami with a 5 W Millennia pump) was used for all fluorescence imaging measurements.

Cell Experiments. MCF-7 cells were cultured at 37 °C in a water-saturated incubator with 5% CO_2. The culture medium was Eagle's Minimum Essential Medium (ATCC, with non-essential amino-acids, 1 mM sodium pyruvate, 2 mM L-glutamine, and 1.5 g/L of sodium bicarbonate) supplemented with 10% (v/v) fetal bovine serum (ATCC) and 1% of penicillin-streptomycin (Cambrex Bio Science). For subculture, the cells were washed twice with PBS and detached by treating with Trypsin-EDTA (ATCC) at 37 °C for 10 min. Newborn calf serum (1 mL, BioWhittaker) was then added at room temperature to inhibit the effect of trypsin. The cells were harvested by centrifugation (1000 rpm, 5 min) and resuspended in the same culture medium.

The cells were plated on a four-chambered Lab-Tek coverglass system (Nalge Nunc) at 50 000 cells per chamber for 24 h, followed by mixing with DOX-HCl and the fullerene-DOX conjugate (both at 230 μM DOX-equivalent) for treatment for 1 h. The living cells were washed carefully with PBS for a complete removal of unattached DOX or conjugate, and the washed cells were kept in PBS for fluorescence imaging. The confocal fluorescence images were obtained with 458 nm excitation, and the two-photon images with femtosecond pulsed laser excitation at 800 nm.

Acknowledgment. Financial support from the NSF (Y.-P.S.) and in part from the NIH (Y.-P.S.) is gratefully acknowledged. L.C. was supported by a Susan G. Komen for the Cure Postdoctoral Fellowship. S.L. was a participant of the summer undergraduate research program jointly sponsored by NSF and Clemson University.

Supporting Information Available: Two videos on Z-stack confocal fluorescence images of free DOX and the conjugate in cells (.AVI files within a .ZIP file). This material is available free of charge via the Internet at http://pubs.acs.org.

REFERENCES AND NOTES

(1) (a) Jensen, A. W.; Wilson, S. R.; Schuster, D. I. *Bioorg. Med. Chem.* **1996**, *4*, 767. (b) Hirsch, A.; Brettreich, M. *Fullerenes: Chemistry and Reactions*, Wiley-VCH: Weinheim, Germany, 2005. (c) Guldi, D. M.; Illescas, B. M.; Atienza, C. M.; Wielopolski, M.; Martín, N. *Chem. Soc. Rev.* **2009**, *38*, 1587.
(2) Lu, F.; Gu, L.; Meziani, M. J.; Wang, X.; Luo, P. G.; Veca, L. M.; Cao, L.; Sun, Y.-P. *Adv. Mater.* **2009**, *21*, 139.
(3) Krusic, P. J.; Wasserman, E.; Keizer, P. N.; Morton, J. R.; Preston, K. F. *Science* **1991**, *254*, 1183.
(4) Markovic, Z.; Trajkovic, V. *Biomaterials* **2008**, *29*, 3561.
(5) Dugan, L. L.; Turetsky, D. M.; Du, C.; Lobner, D.; Wheeler, M.; Almli, C. R.; Shen, C. K. F.; Luh, T. Y.; Choi, D. W.; Lin, T. S. *Proc. Natl. Acad. Sci. U.S.A.* **1997**, *94*, 9434.
(6) Corona-Morales, A. A.; Castell, A.; Escobar, A.; Drucker-Colin, R.; Zhang, L. M. *J. Neurosci. Res.* **2003**, *71*, 121.
(7) Gharbi, N.; Pressac, M.; Hadchouel, M.; Szwarc, H.; Wilson, S. R.; Moussa, F. *Nano Lett.* **2005**, *5*, 2578.
(8) Zakharian, T. Y.; Seryshev, A.; Sitharaman, B.; Gilbert, B. E.; Knight, V.; Wilson, L. J. *J. Am. Chem. Soc.* **2005**, *127*, 12508.
(9) Zacchigna, M.; Klumpp, C.; Prato, M.; Bianco, A. *J. Nanosci. Nanotechnol.* **2009**, *9*, 6210.
(10) Kumar, A.; Patel, G.; Menon, S. K. *Chem. Biol. Drug Des.* **2009**, *73*, 553.

(11) Lu, F.; Haque, S. A.; Yang, S.-T.; Luo, P. G.; Gu, L.; Kitaygorodskiy, A.; Li, H.; Lacher, S.; Sun, Y.-P. *J. Phys. Chem. C* **2009**, *113*, 17768.
(12) Bogdanovic, G.; Kojic, V.; Dordevic, A.; Canadanovic-Brunet, J.; Vojinovic-Miloradov, M.; Baltic, V. V. *Toxicol. in Vitro* **2004**, *18*, 629.
(13) Injac, R.; Perse, M.; Obermajer, N.; Djordjevic-Milic, V.; Prijatelj, M.; Djordjevic, A.; Cerar, A.; Strukelj, B. *Biomaterials* **2008**, *29*, 3451.
(14) Injac, R.; Perse, M.; Cerne, M.; Potocnik, N.; Radic, N.; Govedarica, B.; Djordjevic, A.; Cerar, A.; Strukelj, B. *Biomaterials* **2009**, *30*, 1184.
(15) Heister, E.; Neves, V.; Tilmaciu, C.; Lipert, K.; Beltran, V. S.; Coley, H. M.; Silva, S. R. P.; McFadden, J. *Carbon* **2009**, *47*, 2152.
(16) Ali-Boucetta, H.; Al-Jamal, K. T.; McCarthy, D.; Prato, M.; Bianco, A.; Kostarelos, K. *Chem. Commun.* **2008**, 459.
(17) Chaudhuri, P.; Paraskar, A.; Soni, S.; Mashelkar, R. A.; Sengupta, S. *ACS Nano* **2009**, *3*, 2505.
(18) Liu, Z.; Sun, X.; Nakayama-Ratchford, N.; Dai, H. *ACS Nano* **2007**, *1*, 50.
(19) McNeeley, K. M.; Karathanasis, E.; Annapragada, A. V.; Bellamkonda, R. V. *Biomaterials* **2009**, *30*, 3986.
(20) Gillies, E. R.; Frechet, J. M. J. *Bioconjugate Chem.* **2005**, *16*, 361.
(21) Sun, Y.-P.; Riggs, J. E.; Guo, Z.; Rollins, H. W. In *Optical and Electronic Properties of Fullerenes and Fullerene-Based Materials*; Shinar, J., Vardeny, Z. V., Kafafi, Z. H., Eds.; Marcel Dekker: New York, 1999; p 43.
(22) Martin, R. B.; Fu, K.; Sun, Y.-P. *Chem. Phys. Lett.* **2003**, *375*, 619.
(23) Alwattar, B. H.; Lumb, M. D.; Birks, J. B. In *Organic Molecular Photophysics*; Birks, J. B., Ed.; John Wiley & Sons: London, 1973; Vol. 1, p 403.
(24) Sun, Y.-P.; Wallraff, G. M.; Miller, R. D.; Michl, J. *J. Photochem. Photobiol., A* **1992**, *62*, 333.
(25) Mhawi, A. A.; Fernandes, A. B.; Ottensmeyer, F. P. *J. Struct. Biol.* **2007**, *158*, 80.
(26) Doroshow, J. H. In *Cancer Chemotherapy and Biotherapy: Priciples and Practice*; Chabner, B., Longo, D. L., Eds.; Lippincott Williams & Wilkins: Philadelphia, 2006; p 414.
(27) Banerjee, S. S.; Chen, D. H. *Nanotechnology* **2008**, *19*, 505104.
(28) Helmchen, F.; Denk, W. *Nat. Methods* **2005**, *2*, 932.
(29) König, K. *J. Microsc.* **2000**, *200*, 83.
(30) Xu, C.; Zipfel, W.; Shear, J. B.; Williams, R. M.; Webb, W. W. *Proc. Natl. Acad. Sci. U.S.A.* **1996**, *93*, 10763.
(31) Tewey, K. M.; Rowe, T. C.; Yang, L.; Halligan, B. D.; Liu, L. F. *Science* **1984**, *226*, 466.
(32) Bachur, N. R.; Yu, F.; Johnson, R.; Hickey, R.; Wu, Y.; Malkas, L. *Mol. Pharmacol.* **1992**, *41*, 993.
(33) Lai, B. T.; Gao, J. P.; Lanks, K. W. *Cancer Chemother. Pharmacol.* **1998**, *41*, 155.
(34) Kratz, F.; Beyer, U.; Roth, T.; Tarasova, N.; Collery, P.; Lechenault, F.; Cazabat, A.; Schumacher, P.; Unger, C.; Falken, U. *J. Pharm. Sci.* **1998**, *87*, 338.
(35) Gewirtz, D. A. *Biochem. Pharmacol.* **1999**, *57*, 727.
(36) Tan, W. H.; Wang, K. M.; Drake, T. J. *Curr. Opin. Chem. Biol.* **2004**, *8*, 547.

AM100037Y